Pharmaceutical Research (2023) 40:231–243
https://doi.org/10.1007/s11095-022-03430-8

ORIGINAL RESEARCH ARTICLE

Bone-Targeted Dual Functional Lipid-coated Drug Delivery System for Osteosarcoma Therapy

Jie Zhong[1,2,3] · Weiye Wen[4] · Jinjin Wang[3] · Mengyu Zhang[5] · Yijiang Jia[1] · Xiaowei Ma[6] · Yu-xiong Su[2] · Yuji Wang[1] · Xinmiao Lan[1]

Received: 14 April 2022 / Accepted: 29 October 2022 / Published online: 15 November 2022

Abstract

Purpose or Objective Osteosarcoma is well-known for its high incidence in children and adolescents and long-term bone pain, which seriously reduces the life quality of patients. Cisplatin (CDDP), as the first-line anti-osteosarcoma drug, has been used in many anticancer treatments. At the same time, the serious side effects of platinum (Pt) drugs have also attracted widespread attention. To accurately deliver Pt drugs to the lesion site and realize controlled release of Pt drugs, certain modified delivery systems have been extensively studied.

Methods Among them, liposomes have been approved for clinical cancer treatment due to their highly biocompatibility and superior modifiability. Here, we developed a bone-targeted dual functional lipid-coated drug delivery system, lipid-coated CDDP alendronate nanoparticles (LCA NPs) to target the bone and precisely deliver the drugs to the tumor site. Cell toxicity, apoptosis and cellular uptake were detected to evaluate the anticancer effect for LCA NPs. Furthermore, transwell assay and wound healing assay were conducted to estimate the osteosarcoma cell migration and invasion. Hemolysis assay was utilized to assess the biocapitibility of the kind of NPs.

Results With the aim of bone-targeted unit alendronate (ALD), LCA NPs serve as a rich bone homing Pt delivery system to exert efficient anticancer effects and synergistically reduce bone resorption and bone loss potentially.

Conclusions By providing a highly biocompatible platform for osteosarcoma therapy, LCA NPs may help to significantly enhance the anticancer effect of Pt and greatly reduce the systemic toxicity and side effects of Pt towards osteosarcoma.

Keywords bone target · cisplatin · drug delivery · nanoparticle · osteosarcoma

✉ Yu-xiong Su
richsu@hku.hk

✉ Yuji Wang
wangyuji@ccmu.edu.cn

✉ Xinmiao Lan
xmiao.lan@ccmu.edu.cn

[1] Beijing Area Major Laboratory of Peptide and Small Molecular Drugs, Engineering Research Center of Ministry of Education of China, Beijing Laboratory of Biomedical Materials, School of Pharmaceutical Science, Capital Medical University, Beijing 100069, People's Republic of China

[2] Discipline of Oral and Maxillofacial Surgery, Faculty of Dentistry, The University of Hong Kong, Hong Kong 999077, SAR, China

[3] National Center for Nanoscience and Technology, Chinese Academy of Science, Beijing 100190, People's Republic of China

[4] Department of Stomatology, Beijing Friendship Hospital, Capital Medical University, Beijing 100050, People's Republic of China

[5] National Center for International Research of Bio-Targeting Theranostics, Guangxi Key Laboratory of Bio-Targeting Theranostics, Collaborative Innovation Center for Targeting Tumor Diagnosis and Therapy, Guangxi Talent Highland of Bio-Targeting Theranostics, Guangxi Medical University, Nanning, Guangxi 530021, People's Republic of China

[6] National Center for Veterinary Drug Safety Evaluation, College of Veterinary Medicine, China Agricultural University, Beijing 100193, China

Introduction

Osteosarcoma is a primary malignant bone tumor, which usually occurs in children and adolescents under 20 [1], usually on the surfaces of long bones [2]. The rapid growth of osteosarcoma cells derived from bone-forming mesenchymal cells directly or indirectly form tumor bone-like and bone tissues [3]. Abnormal tissue destruction of cortical bone stimulates nerve endings of the periosteum, thus leading to various kinds of pain [4]. In the middle and late stage of the disease, the patient may also show symptoms such as local lumps and muscular atrophy. It is difficult to detect osteosarcoma in early stage. Meanwhile, rapid disease development, high risk of metastasis and high mortality of osteosarcoma make it difficult to be cured.

CDDP is one of the most widely used chemotherapeutic drugs in clinical practice. CDDP can bind to the DNA of tumor cells and destroy the function of DNA to inhibit mitosis of tumor cells [5]. As a broad-spectrum anticancer drug, CDDP has obvious anti-tumor effects on various malignant cancers including osteosarcoma [6]. However, without any modification, CDDP quickly binds to plasma proteins and loses its cytotoxic efficacy *in vivo*. In addition, Pt drugs have a long half-life and considerable systemic toxicity, especially nephrotoxicity [7], neurotoxicity [8] and severe gastrointestinal reactions [9]. In order to solve the disadvantages of Pt drugs, nanotechnology was utilized to modify drugs, leading to significantly improving the solubility of drugs, reducing the toxicity of drugs and enhancing the targeting ability of drugs. Liposomes are one of the most successful drug delivery systems for clinical translation [10]. At present, liposomal doxorubicin has been approved by the U.S. Food and Drug Administration to treat ovarian cancer, metastatic breast cancer and other tumors [11].

As a drug carrier with good biocompatibility, liposome carrying CDDP into blood can change the distribution and pharmacokinetics of CDDP in human body, thus improving the therapeutic window and reducing the dose and systemic toxicity of CDDP [12]. Some particular modifications to liposomes have been extensively researched in order to improve the targeting ability and triggered releasing ability of CDDP encapsulated liposome, such as adding targeting units and changing lipid composition [13–17]. Due to the slightly acidic environment of the tumor site, some specific pH-sensitive phospholipids have been studied to realize the acid-responsive interactions, and serve as a tumor-environment-responsive nanocarrier [18–20]. The research of targeting bone cancers within bone marrow is ongoing. It remains significantly crucial which targeting ligand binds to that liposome to efficiently deliver the drug to the bone. At present, the reported bone targeting molecules mainly include bisphosphates [21–23], oligopeptides [24, 25], polypropionates [26] and tetracycline-derived agents [27–29]. In recent years, with the development of imaging technology of bone diseases, azido group has been found to have the ability of bone targeting [30]. Bisphosphate, such as alendronate, is the most widely studied bone targeting ligand due to its significant bone-targeting effect and shows good tolerance to the complex chemical environment *in vivo*. In addition, alendronate can also inhibit the activity of osteoclast, delay and reduce bone resorption and bone loss [31, 32]. In this study, we developed a dual functional bone targeting lipid-coated nanoparticle, which coated CDDP with alendronate modified lipids, and simultaneously delivered chemotherapeutic drug – CDDP to exert an influence on bone cancer treatment and play a role in bone repair function with alendronate.

Our previous research demonstrated lipid-coated nano-drug delivery system with specific targeted manners exerts efficient and safe cancer therapy [33, 34]. The nano-drug delivery system designed in this research makes use of the natural bone targeting effect of alendronate [35–37] to effectively deliver lipid-coated nanoparticles loaded with CDDP to the osteosarcoma site, so as to achieve high drug encapsulation rate and improving drug enrichment in lesions. In acidic tumor microenvironment, the CDDP encapsulated in the lipid-coated nanoparticles was released, which increased the cell uptake by osteosarcoma cells, resulting in enhanced cytotoxicity to osteosarcoma cells. Alendronate can not only play an efficient targeting role as a targeting unit, but also as a first-line anti-osteoporosis drug, and can assist CDDP in the treatment of osteosarcoma by reducing bone transformation and promoting bone formation potentially. This study provides a unique dual functional anti-osteosarcoma strategy, which can kill osteosarcoma cells and repair damaged bone tissue at the same time. This bone-targeted lipid-coated nano-drug delivery system (LCA NPs) greatly reduces the side effects of the chemotherapeutic drugs and provides a new idea for chemotherapy of osteosarcoma.

Materials and Methods

Materials

CDDP and ALD were purchased from YuanyeBio (Shanghai, China). Cell counting kit 8 (CCK-8), IGEPAL CO-520, hexanol, cyclohexane and Triton X-100 were purchased from Sigma-Aldrich (Missouri, USA) and used as received without purification. Traut's Reagent was purchased from Sangon Biotech (Shanghai, China). Hydroxyapatite (HAp) was purchased from Macklin (Shanghai, China). 1,2-distearoyl-sn-glycero-3-phosphoethanolamine-N-[maleimide(polyethylene glycol)-2000] (ammonium salt) (DSPE-PEG-Mal) was purchased from Nanocs Incorporation (New York, USA).

1,2-dioleoyl-sn-glycerol-3-phospate (DOPA), 1,2-distearoyl-sn-glycero-3-phosphoethanolamineN-[amino(polyethyleneglycol)-2000] (DSPE-PEG-2000), Cholesterol and 1,2-dioleoyl-3-trimethy-lammonium-propane (DOTAP) were purchased and used as received from Avanti (Alabama, USA). Phosphate buffer saline (PBS), ALP activity kit and Tris–HCl buffer were purchased from Solarbio Life Sciences (Beijing, China). Annexin V-FITC (fluorescein isothiocyanate) apoptosis detection kit was obtained from Keygen Biotech (Nanjing, China). Deionized water (DI water) for all experiments was obtained by a purification system (Milli-Q IQ 7000, Massachusetts, USA).

Synthesis of DSPE-PEG-ALD

ALD was dissolved into Tris–HCl buffer at pH = 8.0 at first, then 20-fold molar Traut's Reagent was added in the former solution. After stirring for 1 h, DSPE-PEG-Mal in the same buffer was added to react for 24 h at room temperature. Then the reaction solution was dialyzed for 3 days using a 500–1000 Da dialysis bag, followed by lyophilization to get the DSPE-PEG-ALD. ^{1}H-Nuclear magnetic resonance spectroscopy (^{1}H-NMR, AVANCE III HD 400, Bruker, Massachusetts, USA) (with MestReNova 9.0 software) and matrix-assisted laser desorption ionization-time of flight mass spectrometry (MALDI-TOF–MS, Autoflex MAX, Bruker Daltonics, Baden-Württemberg, Germany) were utilized to confirm the structure of the drug. The solvent for ^{1}H-NMR was deuteroxide (D_2O).

Fabrication of the LCA NPs

The bone-targeted LCA NPs were synthesized as previously reported [38]. Briefly, CDDP was mixed with silver nitrate and heated at 60℃ for 3 h, followed with stirring overnight. Then the silver chloride was participated using 16,000 × g centrifugal force for 15 min. After centrifugation, the supernatant was filtered using 0.2 μm filter to get the CDDP precursor. The concentration of the Pt was confirmed using inductively coupled plasma mass spectrometry (ICP-MS, NexION 300X, PerkinElmer, Connecticut, USA). Then, 100 μL 200 mM CDDP precursor with 100 μL 20 mM DOPA was added into oil phased consisted of cyclohexane/IGPEL CO-520 (71: 29, V: V). In the meantime, 100 μL 800 mM KCl was added into another oil phase contained cyclohexane/Triton X-100/hexanol (75: 15: 10, V: V). The volume ratio for these two kinds of oil phase should be 3: 1. After 20 min stirring of the two solutions, the solutions were mixed and stirred for another 30 min. Then the same volume of ethanol was added and centrifuged at 16,000 × g to collect the pellets. After three times washing with ethanol, the pellets were resuspended in 3.0 mL chloroform. Then 150 μL 20 mM DOTAP, 150 μL 20 mM cholesterol and 150 μL 10 mM DSPE-PEG-ALD were added into the chloroform. The chloroform was evaporated by rotary evaporation to get the lipid film. After that, 3.0 mL water was added to get the LCA NPs. Liposome extruder (LiposoFast-Basic, Avestin, Ontario, Canada) with 0.22 μm membrane (Whatman, Buckinghamshire, UK) was used to get the uniform NPs. To measure the final concentration in LCA NPs, NPs were demulsificated using 1: 1 methanol first, followed by detection using ICP-MS.

Characterization of the NPs

The diameter and zeta potential were determined using dynamic light scattering (DLS, Zetasizer nano SZ90, Malvern, Cambridge, UK). Furthermore, the morphology of the NPs was detected by transmission electron microscopy (TEM, Tecnai G2 20 S-TWIN, FEI, Oregon, USA). For preparing the samples for TEM detection, NPs were diluted and then doped on carbon grid. After negative stained with 2% uranyl acetate, the morphology was characterized using TEM.

HAp Binding Ability

To detect the binding ability of the NPs, two kinds of NPs were fabricated. One of the NPs were synthesized using DSPE-PEG-2000 (LCC NPs), while the other one fabricated using DSPE-PEG-ALD (LCA NPs). 0.4% Rhodamine PE was added into the NPs while fabricating. For HAp binding test, the NPs were dispersed in DI water at the concentration of 2 mg/mL first. Then the two NPs were incubated with 10 mg/mL HAp for 24 h. HAp was centrifuged at 4000 rpm for 10 min before detection using microplate reader. The residual fluorescence of the two NPs was detected with excitation wavelength at 540 nm and emission wavelength at 625 nm.

Cell Culture

Osteosarcoma cell lines (MG63 and U2OS) and pharynx squamous cell carcinoma cell line (FaDu) were bought from ATCC (Virginia, USA). MG63 cell line was cultured with Eagle's Minimum Essential Medium (EMEM, Wisent, Nanjing, China) supplemented with 10% (v/v) heat-inactivated fetal bovine serum (FBS, Wisent, China) and 1% penicillin – streptomycin (v/v) (P/S, Wisent, China). U2OS cell line was maintained in McCoy 5A medium (Wisent, China), with 10% FBS and 1% P/S. FaDu cell line was cultured with Dulbecco's Modified Eagle Medium (DMEM, Wisent, Nanjing, China) supplemented with 10% FBS and 1% P/S. PBS (cell culture grade) for all cell culture tests was purchased from Meilunbio (Liaoning, China). All the cell lines were cultured in a humified atmosphere containing 5% CO_2.

Cell Viability

Cell toxicity of the drugs *in vitro* was estimated by MG63, U2OS and FaDu. Briefly, MG63 and U2OS cells were inoculated into 96-well plates at a density of 5×10^3 cells/well and adhered overnight. CDDP, CDDP + ALD, LCA NPs were added into the 96-well plate based on a consistent Pt concentration, and the concentration of ALD group was based on the ALD containing in the LCA NPs. Meanwhile, to obtain cell viability curves and IC_{50} values of each group, a series of concentration gradients of Pt (0, 0.1, 1, 10, 50, 100 μM) were set. In detail, 96-well plates were incubated in the incubator for a further 24 h. The medium was carefully aspirated and discarded. To each well, medium containing 10% CCK-8 was added to the cells. The absorbance at 450 nm was measured with a microplate reader.

Cellular Pt Uptake

The two osteosarcoma cell lines (MG63 and U2OS) and a pharynx squamous cell carcinoma cell line (FaDu) were seeded into 24-well plate, with a density at 2.5×10^5 cells per well. Cell lines were treated with the groups containing consistent Pt concentration, 10 μM Pt at 37℃. After 4 h incubation, cells were washed twice with PBS and digested with 75% HNO_3 and 25% HCl. At last, the Pt uptake by cells were determined using ICP-MS.

Cell Apoptosis

For apoptosis detection, MG63 and U2OS cell lines were seeded into a six-well plate followed by treated with 10 μM Pt at 37℃ for 4 h. The ALD concentration was determined according to Pt concentration in all the groups. After collection of the cells, they were incubated with Annexin V and propidium iodide (PI) according to manufacturer's protocol. The data was collected using BD Accuri™ C6 Plus Flow Cytometer (BD Bioscience, New Jercy, USA) and analyzed by FlowJo software.

Cell Invasion Assay

Cell invasion was determined using transwell with 8 μm polycarbonate membrane chambers (Corning, New York, USA). Briefly, 100 μL serum-free medium was added into the upper chamber first, then 200 μL cells at a density of 2.5×10^5 cells per mL in serum-free medium was added into the upper chamber. 750 μL complete medium was added into lower chamber afterwards. After that, cells with different treatment groups were incubated for 24 h. Then the upper chamber was washed by PBS and fixed using 3.7% formaldehyde solution. At last, crystal violet was used to stain the cells invaded through the membrane.

Wound Healing Assay

Wound healing assay was performed to detect the migration ability of osteosarcoma cell lines. Cells were seeded in a six-well plate for adhesion. Then the adhesion cells were scraped a 1 mm wound by pipette tips and then washed with PBS. After that, cells were treated using 0.1 μM Pt for MG63 cell line and 1 μM Pt for U2OS cell line. Images were captured after 48 h treatment and the wound was calculated to evaluate the cell migration.

Hemolysis Ability

Mice whole blood was collected and then centrifuged at 10,000 × g for 5 min to collect the red blood cells. And the red blood cells were washed with PBS for three times before being incubated with drugs. CDDP, ALD, CDDP with ALD, and LCA NPs at 10 μM were incubated with the red blood cells to see whether they could lead to hemolysis. PBS with 0.1% Triton X-100 was treated as a positive control. After 4 h incubation, all the groups were centrifuged, and the supernatant were utilized to detect the OD value at 577 nm.

Statistical Analysis

All data were presented as the mean ± SD. Data analysis of variance was performed using GraphPad Prism 8.0 (China) and Origin 2018 (Origin Lab, USA) using one-way ANOVA and multiple t-test. P-value < 0.05 will be considered statistically significant.

Results and Discussions

Synthesis of the DSPE-PEG-ALD

Systemic gene delivery by non-viral vectors offers various benefits, especially in terms of security(39). The FDA has given the go-ahead for clinical studies for lipid-based gene carriers, which are among the most frequently used non-viral vectors, especially during the COVID-19 global pandemic [40, 41]. For fabrication of bone-targeted lipid-coated drug delivery system, ALD was sulfhydrylated using Traut's Reagent (2-Iminothiolane) first. Traut's Reagent could introduce sulfhydryl group (-SH) to ALD while reacting with the primary amine group (-NH2) in ALD. Then DSPE-PEG-Mal reacted with thiolated ALD to get the DSPE-PEG-ALD. The chemical reaction progress was illustrated in Fig. 1A. The chemical structure of synthesized DSPE-PEG-ALD was determined using ^{1}H-NMR (Fig. 1B). ALD had a distinctive signal for CH_2 protons at 2.0 ppm (b, c in Fig. 1B), which was also seen in the spectra of DSPE-PEG-ALD while cannot be found in DSPE-PEG-Mal. Also, other characteristic

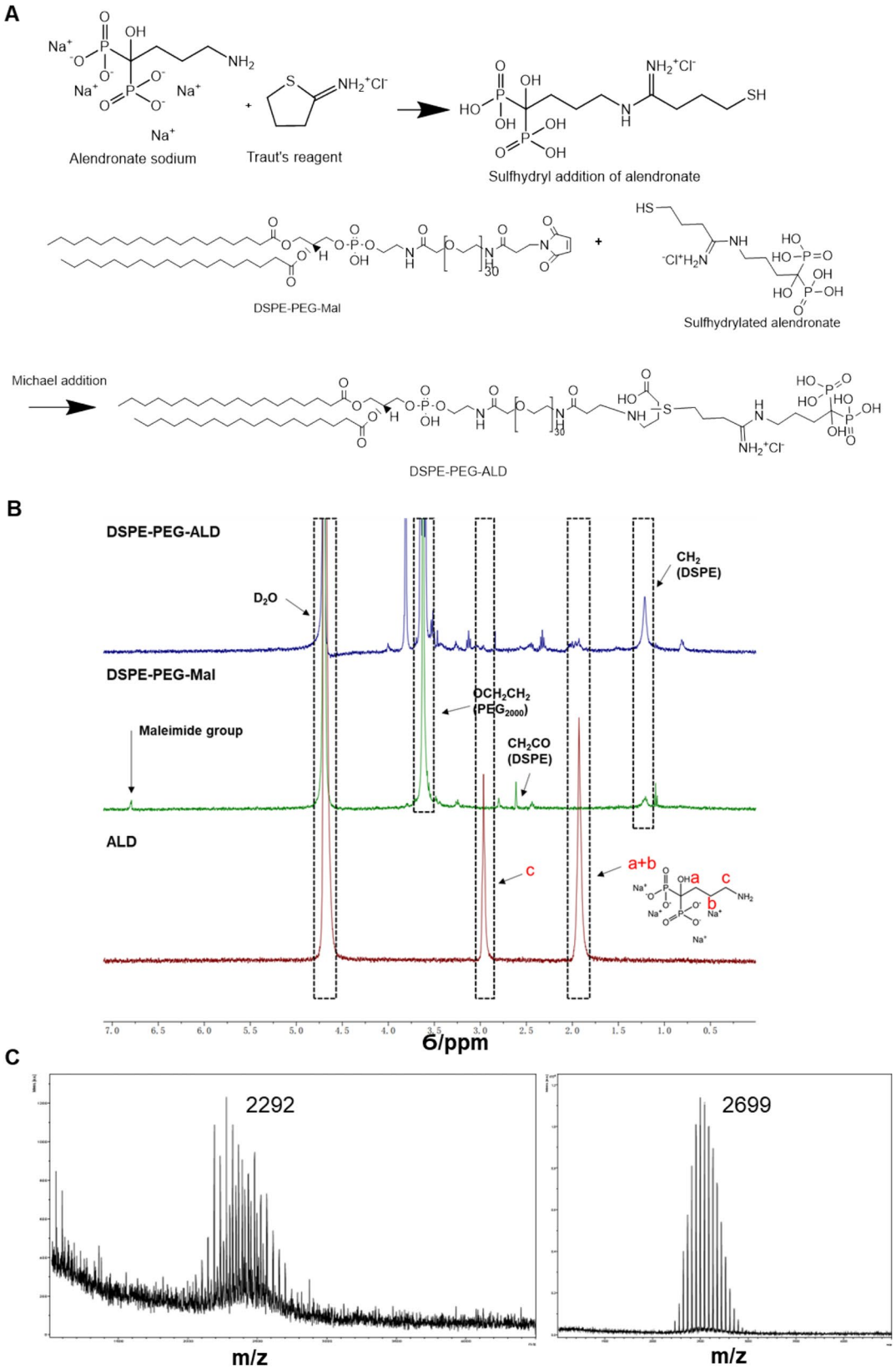

Fig. 1 Conjugation of ALD with 1,2-distearoyl-sn-glycero-3-phosphoethanolamineN-[amino(polyethyleneglycol)-2000] (DSPE-PEG-2000). (**A**) Chemical reaction of the synthesis process. (**B**) Characterization of DSPE-PEG-ALD using ^{1}H-NMR. (**C**) Mass spectrum confirmation of DSPE-PEG-ALD determined by MALDI-TOF.

peak of ALD (a in Fig. 1B) can be found in DSPE-PEG-ALD,. Additionally, the exact mass of the DSPE-PEG-ALD was confirmed using MALDI-TOF (Fig. 1C). The exact mass for DSPE-PEG-Mal and DSPE-PEG-ALD were calculated by ChemDraw, they were 2292 and 2699 respectively. These results were convinced with the result of mass spectrum. ^{1}H-NMR and MALDI-TOF demonstrated the successful conjugation for ALD with DSPE-PEG-Mal.

Fabrication of the LCA NPs

LCA NPs were fabricated to combine the chemotherapeutic agent, CDDP, and the bisphosphonate agent, ALD. The synthesis process of the NP was exhibited in Fig. 2A and B. Firstly, a CDDP precursor, cis-$[Pt(NH_3)_2(H_2O)_2]_2(NO_3)_2$ was prepared to enhance the poor solubility of CDDP. Water in oil in water phase was utilized to prepare the micro-emulsion for the whole reaction. The well-prepared bone-targeted NP could target bone by DSPE-PEG-ALD first. In most cases, the presence of PEG aids in reducing nonspecific interaction to increase circulation time [39]. Furthermore, DOTAP and cholesterol on the outer lipid layer could contribute to cell membrane interaction, endosome escape and reduce systemic cytotoxicity respectively. DOPA was the main composition in the inner layer of LCA NPs. DOPA, as a neutral "helper lipid", could enhance deliver efficiency and regulate the size of the NPs [42, 43]. The average diameter of NPs detected using DLS was 144.4 ± 20.23 nm with the uniform polydispersity index (PDI) value less than 0.1 (Fig. 2C). The zeta potential distribution was $+47 \pm 9.33$ mV, indicating the NPs were cationic liposome. Additionally, the morphology of the negative stained NPs was captured using TEM. As shown in Fig. 2D, NPs presented as spherical shape with a diameter around 120 nm. Lipid-coated cisplatin NPs (LCC-NPs) was synthesized as a control group to further confirm the targeting ability of ALD. TEM and DLS demonstrated that there is no significant difference for characterization of LCA-NPs and LCC-NPs. The size and zeta potential of the two kinds of NPs were almost the same. In sum, we successfully synthesized a uniform distributed lipid-coated NPs loaded with CDDP and ALD, which could target bone and further be applied for osteosarcoma therapy.

Cellular Uptake

In osteoblastic or osteoblastic-like cells, it has been suggested that ALD conjugation on particles may boost their cellular accumulation and help distribute in the bone compared to the other tissue [22, 44]. To determine the Pt uptake ability of the drugs, cells in 24-well plate were treated for 24 h at the same concentration of Pt, and then the cells were digested using hydrochloric acid and nitric acid followed by ICP-MS detection (Fig. 3A). For MG63 cell lines, nearly 250 ng Pt in LCA NPs group was uptaken per well, while only 50 ng, 70 ng and 120 ng for CDDP, CDDP with ALD and LCA NPs respectively. In addition, we also demonstrated the uptake ability using U2OS cell line. More Pt uptake was found in LCA NPs group for this cell line. Furthermore, in order to further confirm the specific targeting ability of ALD in osteosarcoma cell lines, we check the cellular uptake of the four groups in a kind of nasopharyngeal carcinoma, name FaDu cell lines. We found that LCA NPs cannot be taken more by FaDu cell lines. In sum, we can confirm that lipid coating can help tumor cells get more Pt, while the LCA NPs can be more easily to be uptake by osteosarcoma cell lines, which is one of the most important properties for cancer therapy.

HAp Binding Ability

In addition to being a bone cell-seeking molecule, bisphosphonates (such as ALD) which have a strong affinity for the surfaces of calcium phosphate, can specifically target bone mineral and act as powerful inhibitors of osteoclast-mediated bone resorption [21–23, 45]. Since bone microenvironment is rich in hydroxyapatite (HAp), the effects of bisphosphonates on natural bone mineral have previously been modelled using synthetic HAp. The binding affinity of the detection of NPs for HAp can represent the targeting ability of the NPs to the bone site to a certain extent. The schematic illustration of ALD-modified NPs for bone mineral target is shown in Fig. 3B.

In order to further warrant the bone mineral target property of the LCA NPs for future possible *in vivo* study, two kinds of NPs with different lipid coating were fabricated. Moreover, fluorescence was added into the two kinds of NPs. LCA NPs were coated with DSPE-PEG-ALD we synthesized, while LCC NPs were coated with DSPE-PEG-2000. As shown in Fig. 3C, the residual fluorescence in the supernatant was determined and we found that significantly less fluorescence was detected in LCA NPs groups, which means more fluorescence was bonded with HAp. With ALD modification, the HAp binding affinity of LCA NPs was significantly increased to 50% compared to non-modified NPs, confirming the favorable bong targeting potential. We can conclude from this result that LCA NPs can target bone site for further osteosarcoma therapy.

Anticancer Effects *In Vitro*

Due to excellent cellular uptake and bone-targeted properties as shown in Fig. 3, NPs may exert anticancer effects *in vitro*. The anticancer functions were further tested by calculating the cell viability and IC_{50} of a pharynx squamous cell carcinoma cell line, FaDu and two osteosarcoma cell lines, MG63 and U2OS. After treatment with LCA NPs, more

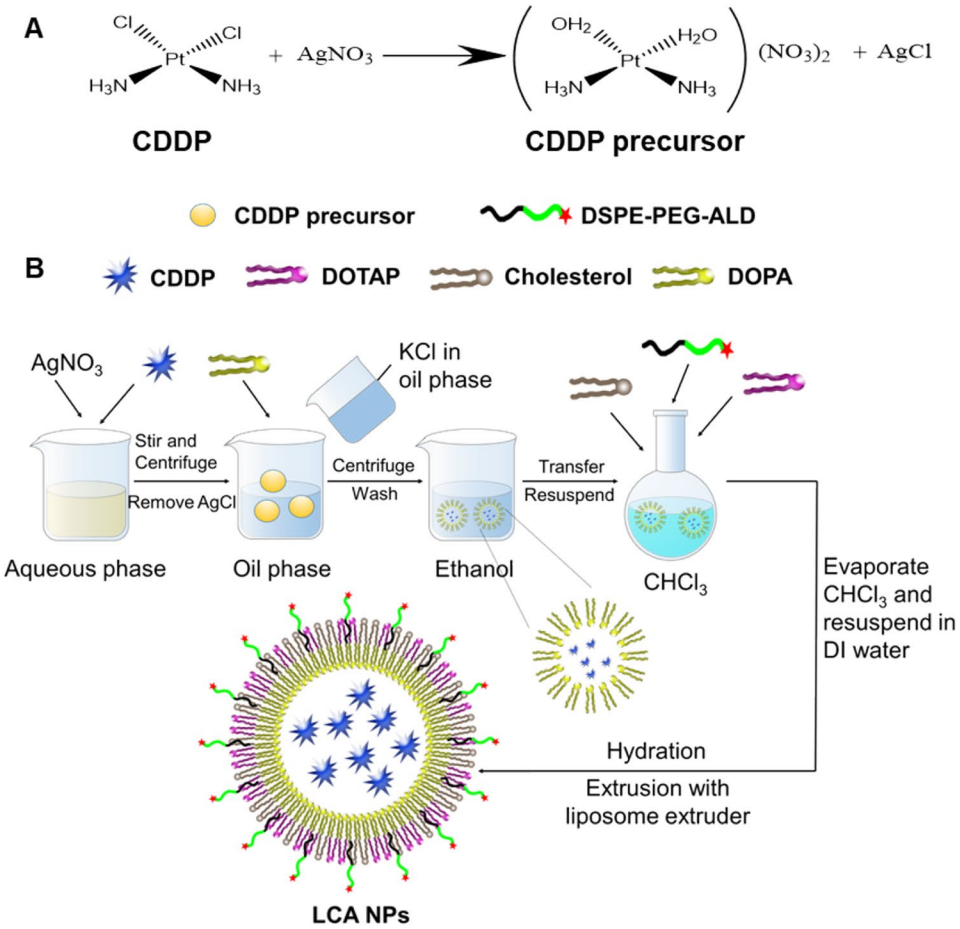

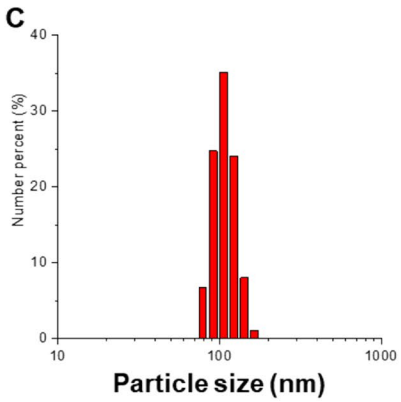

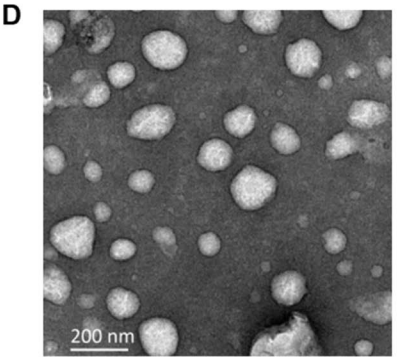

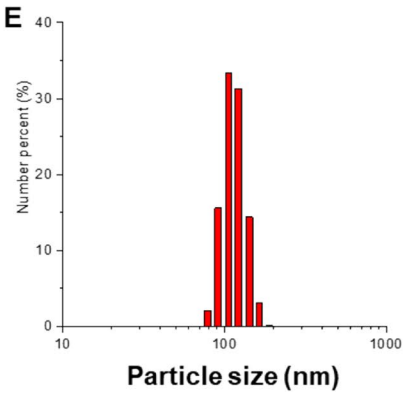

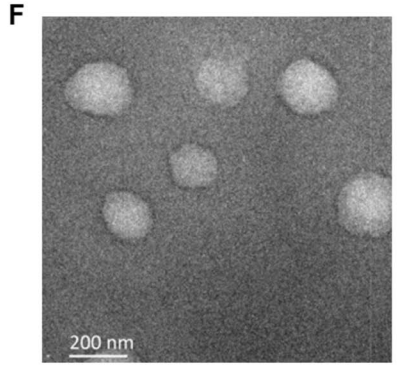

Fig. 2 Synthesis and characterization of NPs. (**A**) The chemical reaction of the CDDP precursor. (**B**) Schematic illustration of synthesis process of the NPs. (**C**) Size distribution of LCA-NPs detected using DLS. (**D**) Representative images of the LCA-NPs characterized using TEM. (**E**) Size distribution of LCC-NPs detected using DLS. (**F**) Representative images of the LCC-NPs characterized using TEM.

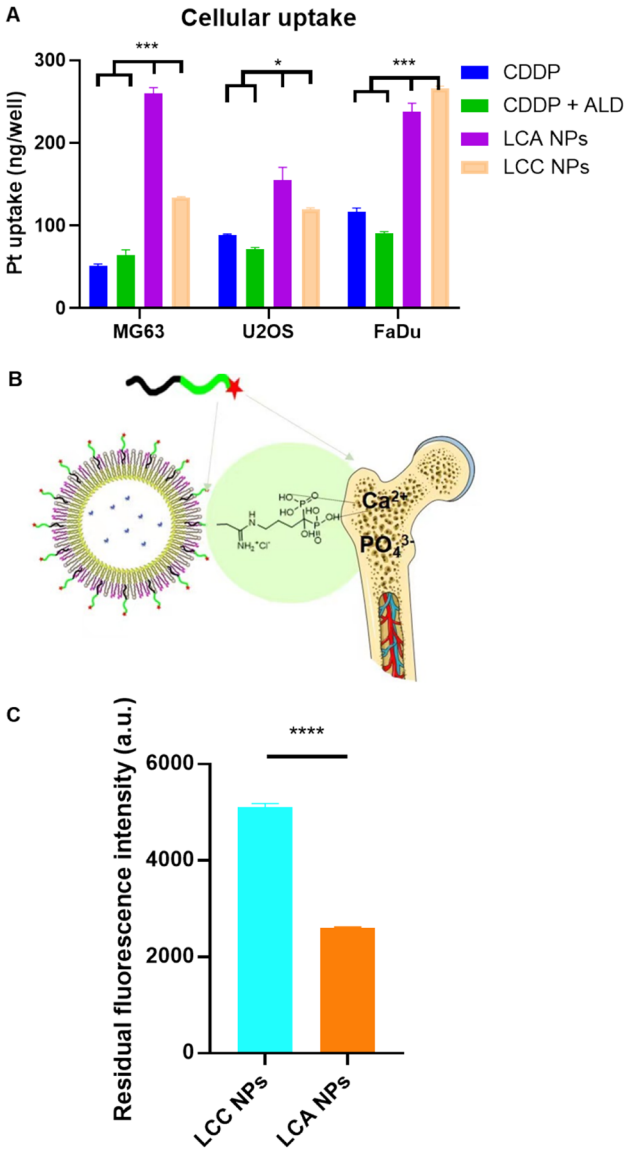

Fig. 3 Cellular uptake and bone-targeted property of the NPs (**A**) Cellular uptake of the three cell lines for 24 h. The p-value was determined using one-way ANOVA. (*$p < 0.05$, ***$p < 0.001$); (**B**) Schematic illustration of ALD-modified NPs for bone mineral targeting; (**C**) HAp binding affinity represented using residual fluorescence intensity. The variance was conducted by t-test (****$p < 0.0001$).

than 99% of MG63 and U2OS cells were killed at a 10 µM concentration of Pt (Fig. 4A, B). Compared to the Pt alone group, LCA NPs significantly increased the cytotoxicity of Pt drugs to more than twofold than CDDP. Moreover, IC_{50} was significantly decreased in three cell lines after treatment of lipid coated NPs (Fig. 4C), which indicated that lipid coated NPs may help avoid severe systemic side effects of Pt. To be specific, IC_{50} was significantly decreased in LCA NPs than LCC NPs for osteosarcoma, while LCA showed distinguished efficiency in nasopharyngeal carcinoma. This further confirmed the targeting ability of ALD. Meanwhile, no significant cytotoxicity of LCA NPs was observed compared to the LCC NPs in the FaDu cell line. Here, we can make a conclusion that LCA NPs could be expected to be a safe and effective anticancer nano-drug system after further verification, which could be a promising powerful tool for osteosarcoma therapy.

Cell Apoptosis

As a programmed cell death process, apoptosis regulates the destruction of a cell. Apoptosis assay is an significant property in anticancer drug treatment [46].

Cell apoptosis was detected using flow cytometry by Annexin V-PI kit. Annexin V can bind to phosphatidylserine, while PI can stain DNA in dead cell nucleus. Thus cells stained with Annexin V but PI negative can be recognized as early apoptosis cells. U2OS cell line was treated with 10 µM Pt for 4 h, and the results analyzed by FlowJo was presented in Fig. 5. 17.8% early apoptosis cells were detected in LCA NPs treated group, while few apoptosis was found in other groups. This demonstrated LCA NPs could promote apoptosis of U2OS cell line, thus further exerting promising favorable anti-cancer effect.

However, there were few limitations to our study. The anticancer effects and mechanism of LCA NPs were not investigated *in vivo*. LCA NPs have to be studied more in animal models, and research into the underlying processes that invasion inhibition and apoptosis induction *in vivo* is necessary.

Cell Invasion and Migration

One of the primary causes of morbidity and death in patients with osteosarcoma is distant metastasis [47]. As a result, transwell invasion assay and wound healing assay were performed to investigate the influence of LCA NPs on MG63 and U2OS cell lines as described in previous studies [48, 49].

Cell invasion and migration were performed using 8 µm membrane transwell and wound healing assay. First of all, cells were seeded into the upper chamber of the transwell, while some of them can invade into the lower membrane of the chamber. After scrapped out the upper chamber cells, migrated cells were captured and counted. As it is shown in Fig. 6A and D, all the groups with treatment can induce cell invasion. CDDP and ALD could accelerate cell invasion, while LCA NPs induced a minimum of invaded cell among them. Additionally, wound healing assay was conducted to reveal the cell migration ability. Attached cells were scratched and treated for 48 h. Represented images of the two cell lines after treatment for 48 h for different groups were shown in Fig. 6B and C. Moreover, quantitative analysis was performed according to the images. Cell lines treated with CDDP and ALD migrated even more than

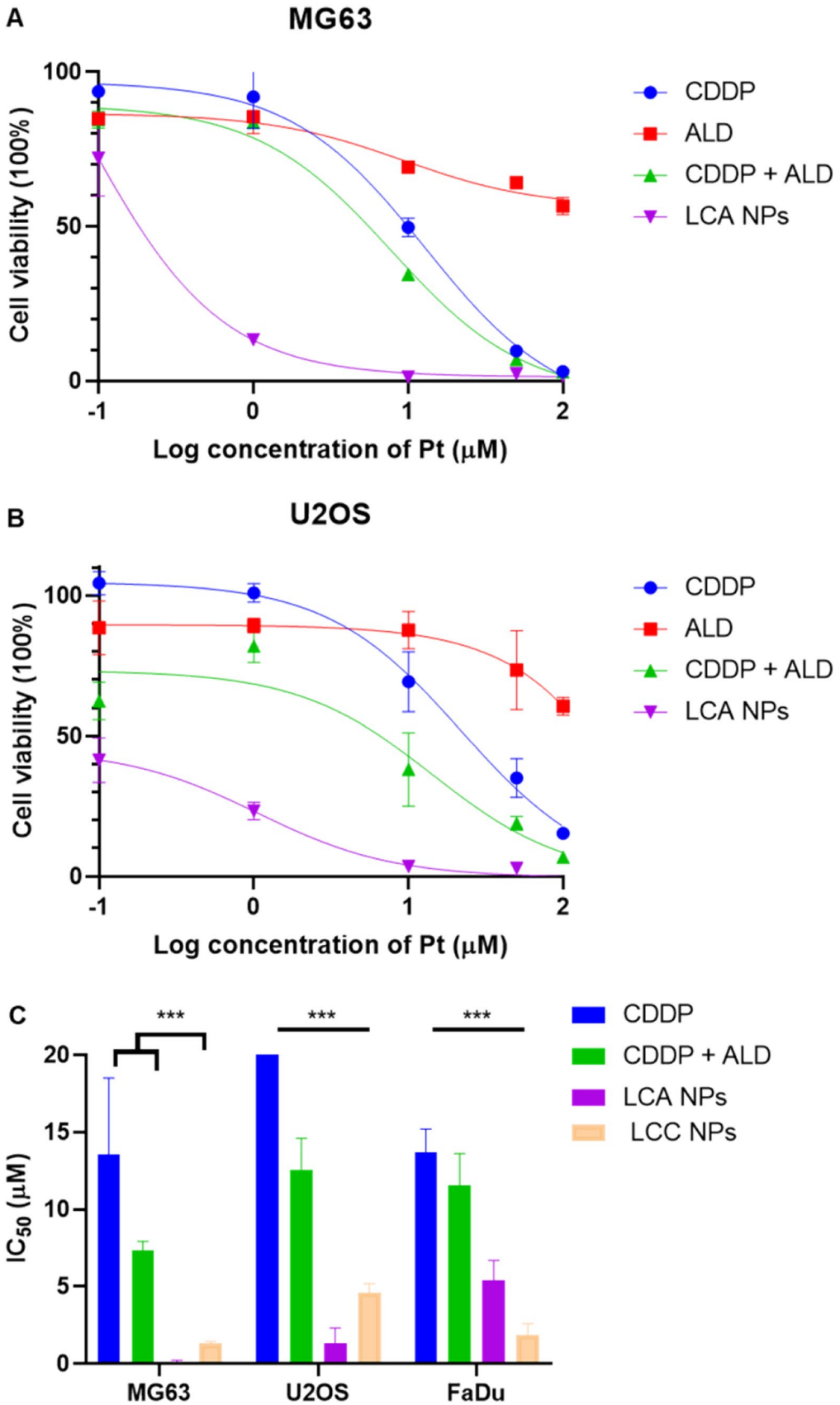

Fig. 4 Anti-cancer effect of the LCA NPs towards osteosarcoma cell lines *in vitro*. Cell viability of different osteosarcoma cell lines, (**A**) MG63 and (**B**) U2OS. (**C**) IC_{50} concentration of the drugs treating for three cell lines. The variance analysis was conducted using group to group t-test (***$p < 0.001$). The Pt concentration of the drugs was determined by ICP-MS.

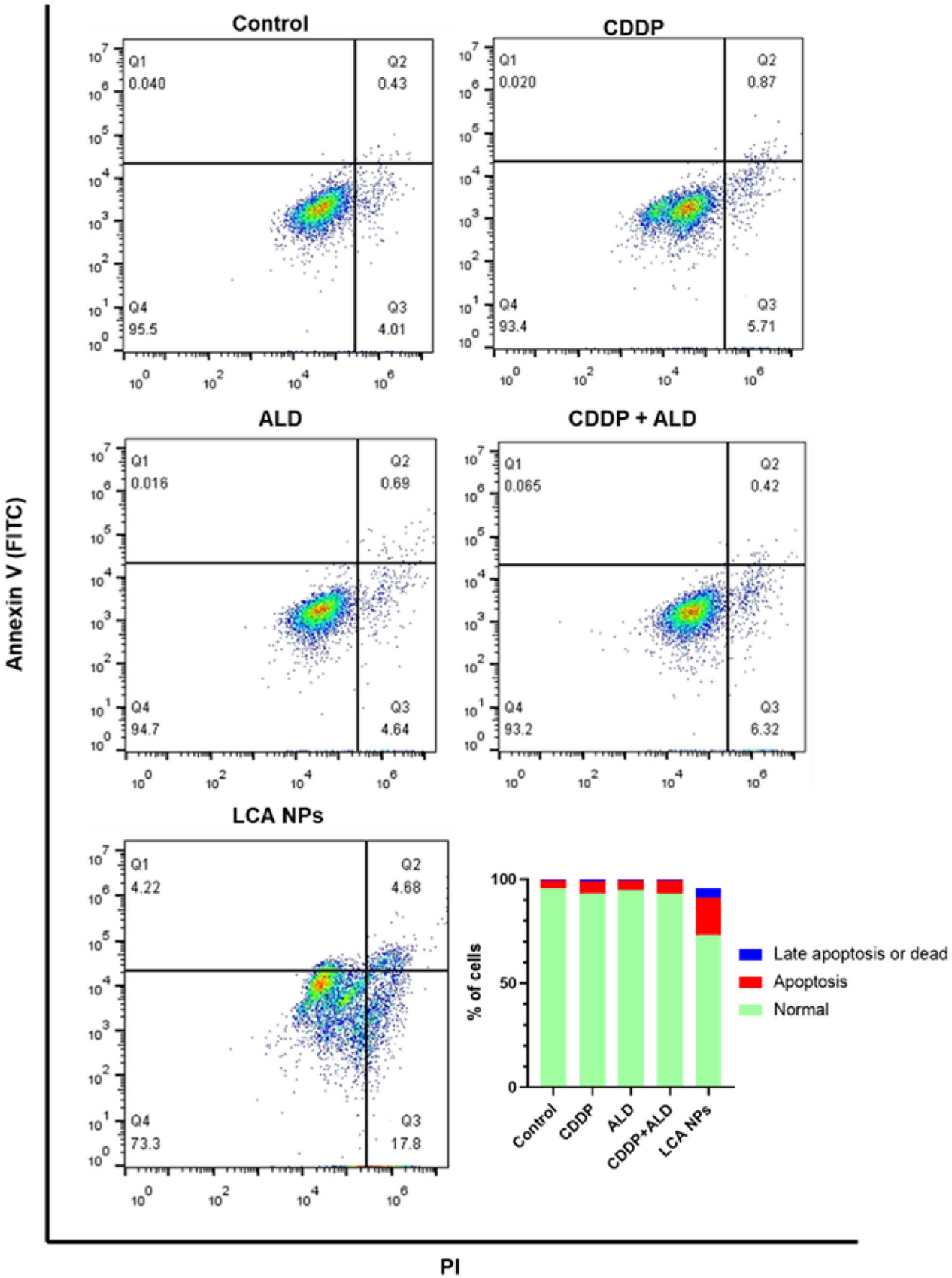

Fig. 5 Cell apoptosis analysis of U2OS cell by flow cytometry.

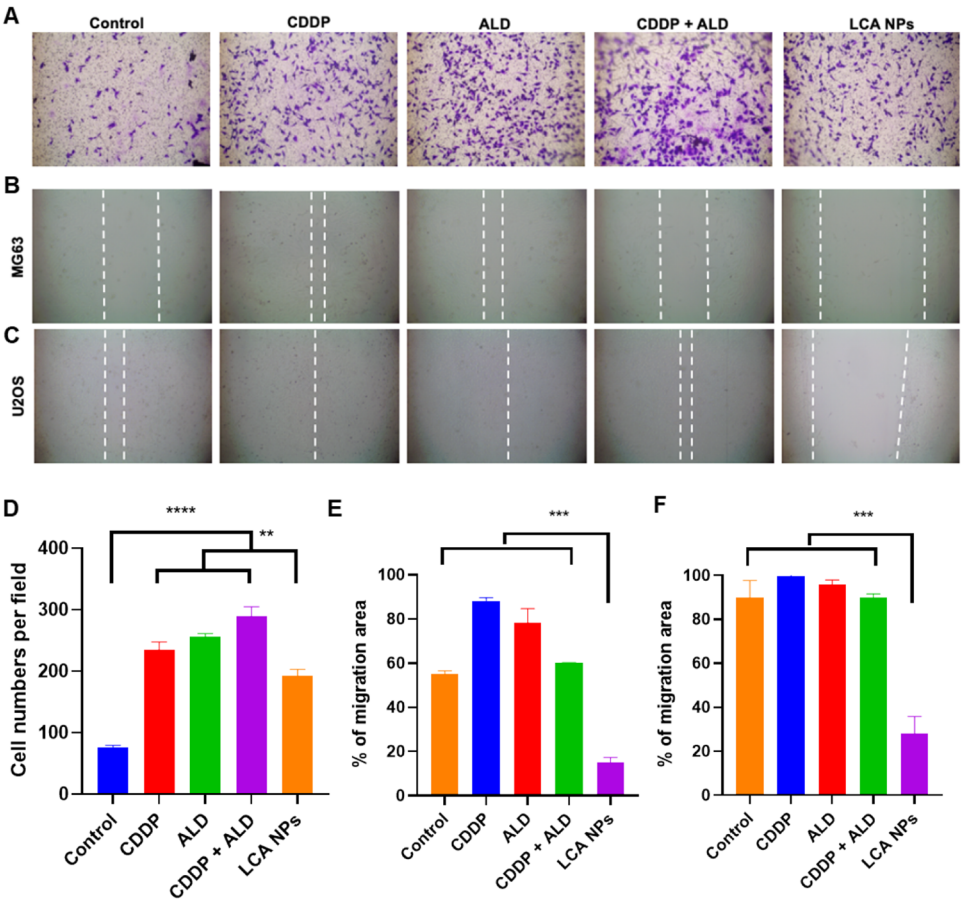

Fig. 6 Cell invasion and migration. (**A**) Represented images invaded cells; Wound healing assay performed on (**B**) MG63 and (**C**) U2OS cell lines; (**D**) (**E**)(**F**) Quantitative analysis of (**A**)(**B**)(**C**). Statistical analysis was performed using one-way ANOVA. (**p < 0.01, ***p < 0.001, ****p < 0.0001).

control group, which indicated that chemotherapeutic and bisphosphonate drugs could induce cell migration. Briefly combining CDDP and ALD could delay migration to some extent. Furthermore, LCA NPs showed the most significant inhibition rate among all the groups. Taken together, based on the aforementioned data, LCA NPs could significantly prohibit cell invasion and migration, which provides a promising treatment strategy for osteosarcoma.

Biosafety of the Drugs

Although the excellent cytotoxicity of chemotherapeutic drugs is needed for cancer treatment, the biosafety is also important for drugs. One of the weaknesses for CDDP is nonnegligible systemic toxicity it caused. Whether drugs can cause hemolysis can be recognized as a criterion for biosafety [50]. The red blood cells were incubated with different drugs for 4 h. OD value at 577 nm of the supernatant was detected to evaluate the hemolysis (Fig. 7). It has been found that the hemolysis in LCA NPs was significantly lower than any other groups, while no significant difference was detected compared to negative control. In this part,

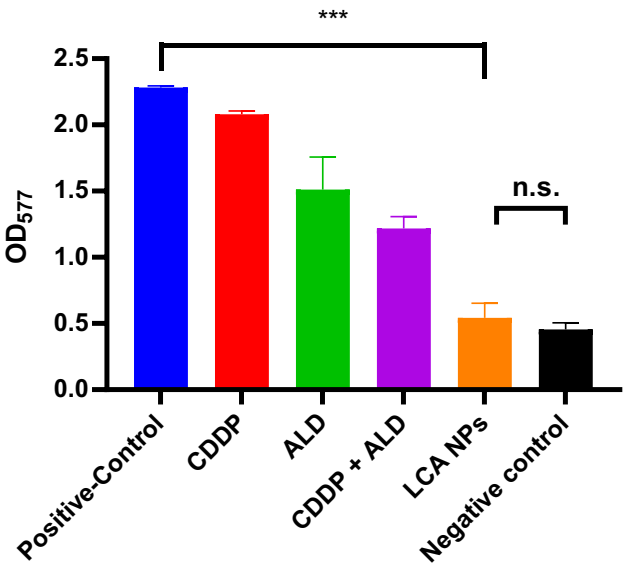

Fig. 7 Hemolysis ability of the drugs. OD value at 577 nm of red blood cells after 4 h incubation with drugs. (*** p < 0.001, n.s., no significant difference).

biocompatibility was evaluated by hemolysis assay. Based on the all previous data, it can be concluded that LCA NPs enhanced Pt drug accumulation in tumor cells without bringing obvious cytotoxicity.

Conclusions

In this project, ALD was conjugated with DSPE-PEG-2000 to realize the bone target property of the NPs. CDDP was encapsulated into a lipid inner layer to enhance its solubility and significantly boosted the anti-cancer effect, including increased cancer cell toxicity supplemented with less migration and invasion. The design of this delivery system not only fully played the targeting advantages and potential bone repair ability of ALD, but also provided a new idea for improving the solubility and bioavailability of CDDP. In the meanwhile, the biosafety of LCA NPs can be promised. In sum, a bone-targeted lipid coated CDDP NP was successfully fabricated. We can conclude that LCA NPs can be utilized as an effective and safe chemotherapeutic agent for osteosarcoma therapy, although the systematic *in vivo* test and the overall bone-targeting metabolism need to be considered in the future.

Acknowledgements This work was supported by the Beijing Municipal Colleges and Universities High Level Talents Introduction and Cultivate Project-Beijing Great Wall Scholar Program (CIT&TCD 20180332, China) and Chinese National Natural Science Foundation project (Grant No. 31971312, 32171389).

Author Contributions Jie Zhong and Xinmiao Lan contributed to conceiving and designing the project, performing the experiment, data analysis, interpretation, and drafting the manuscript. Weiye Wen, Jinjin Wang, Yijing Jia, and Mengyu Zhang contributed to data acquisition. Xiaowei Ma, Yu-xiong Su and Yuji Wang contributed to design and data interpretation, critically revised the manuscript. All authors gave final approval and agree to be accountable for all aspects of the work.

Declarations

Conflict of Interest There are no conflicts to declare.

References

1. Ottaviani G, Jaffe N. The epidemiology of osteosarcoma. In: Jaffe N, Bruland OS, Bielack S, editors. Pediatric and Adolescent Osteosarcoma. Boston, MA: Springer, US; 2010. p. 3–13.
2. Schajowicz F, McGuire MH, Santini Araujo E, Muscolo DL, Gitelis S. Osteosarcomas arising on the surfaces of long bones. J Bone Joint Surg Am. 1988;70(4):555–64.
3. Prater S, McKeon B. Osteosarcoma: StatPearls Publishing, Treasure Island (FL); 2020.
4. Fan TM, de Lorimier LP, O'Dell-Anderson K, Lacoste HI, Charney SC. Single-agent pamidronate for palliative therapy of canine appendicular osteosarcoma bone pain. J Vet Intern Med. 2007;21(3):431–9.
5. Dasari S, Tchounwou PB. Cisplatin in cancer therapy: molecular mechanisms of action. Eur J Pharmacol. 2014;740:364–78.
6. Isakoff MS, Bielack SS, Meltzer P, Gorlick R. Osteosarcoma: Current treatment and a collaborative pathway to success. J Clin Oncol. 2015;33(27):3029–35.
7. Yao X, Panichpisal K, Kurtzman N, Nugent K. Cisplatin Nephrotoxicity: A Review. Am J Med Sci. 2007;334(2):115–24.
8. Gregg RW, Molepo JM, Monpetit VJ, Mikael NZ, Redmond D, Gadia M, Stewart DJ. Cisplatin neurotoxicity: the relationship between dosage, time, and platinum concentration in neurologic tissues, and morphologic evidence of toxicity. J Clin Oncol. 1992;10(5):795–803.
9. Shahid F, Farooqui Z, Khan F. Cisplatin-induced gastrointestinal toxicity: An update on possible mechanisms and on available gastroprotective strategies. Eur J Pharmacol. 2018;827:49–57.
10. Allen TM, Cullis PR. Liposomal drug delivery systems: from concept to clinical applications. Adv Drug Deliv Rev. 2013;65(1):36–48.
11. Barenholz Y. Doxil®–the first FDA-approved nano-drug: lessons learned. J Control Release. 2012;160(2):117–34.
12. Irby D, Du C, Li F. Lipid-drug conjugate for enhancing drug delivery. Mol Pharm. 2017;14(5):1325–38.
13. Iinuma H, Maruyama K, Okinaga K, Sasaki K, Sekine T, Ishida O, Ogiwara N, Johkura K, Yonemura Y. Intracellular targeting therapy of cisplatin-encapsulated transferrin-polyethylene glycol liposome on peritoneal dissemination of gastric cancer. Int J Cancer. 2002;99(1):130–7.
14. Schroeder A, Honen R, Turjeman K, Gabizon A, Kost J, Barenholz Y. Ultrasound triggered release of cisplatin from liposomes in murine tumors. J Control Release. 2009;137(1):63–8.
15. Gu T-T, Li C, Xu Y, Zhang L, Shan X, Huang X, Guo L, Chen K, Wang X, Ge H, Ning X. Stimuli-responsive combination therapy of cisplatin and Nrf2 siRNA for improving antitumor treatment of osteosarcoma. Nano Res. 2020;13(3):630–7.
16. Chen J, Wang X, Yuan Y, Chen H, Zhang L, Xiao H, Chen J, Zhao Y, Chang J, Guo W, Liang XJ. Exploiting the acquired vulnerability of cisplatin-resistant tumors with a hypoxia-amplifying DNA repair-inhibiting (HYDRI) nanomedicine. Sci Adv. 2021;7(13).
17. Yang Y, Liu X, Ma W, Xu Q, Chen G, Wang Y, Xiao H, Li N, Liang XJ, Yu M, Yu Z. Light-activatable liposomes for repetitive on-demand drug release and immunopotentiation in hypoxic tumor therapy. Biomaterials. 2021;265: 120456.
18. Yatvin MB, Kreutz W, Horwitz BA, Shinitzky M. pH-sensitive liposomes: possible clinical implications. Science. 1980;210(4475):1253–5.
19. Navon Y, Radavidson H, Putaux JL, Jean B, Heux L. pH-sensitive interactions between cellulose nanocrystals and DOPC liposomes. Biomacromol. 2017;18(9):2918–27.
20. dos Santos GC, de Oliveira Reis EC, Ribeiro Rocha TG, Leite EA, Lacerda RG, Ramaldes GA, de Oliveira MC. Study of the pilot production process of long-circulating and pH-sensitive liposomes containing cisplatin. J Liposome Res. 2011;21(1):60–9.
21. Swami A, Reagan MR, Basto P, Mishima Y, Kamaly N, Glavey S, Zhang S, Moschetta M, Seevaratnam D, Zhang Y, Liu J, Memarzadeh M, Wu J, Manier S, Shi J, Bertrand N, Lu ZN, Nagano K, Baron R, Sacco A, Roccaro AM, Farokhzad OC, Ghobrial IM. Engineered nanomedicine for myeloma and bone microenvironment targeting. Proc Natl Acad Sci U S A. 2014;111(28):10287–92.
22. Nguyen TDT, Pitchaimani A, Aryal S. Engineered nanomedicine with alendronic acid corona improves targeting to osteosarcoma. Sci Rep. 2016;6(1):36707.
23. Chen Q, Zheng C, Li Y, Bian S, Pan H, Zhao X, Lu WW. Bone targeted delivery of SDF-1 via alendronate functionalized nanoparticles in guiding stem cell migration. ACS Appl Mater Interfaces. 2018;10(28):23700–10.

24. Sekido T, Sakura N, Higashi Y, Miya K, Nitta Y, Nomura M, Sawanishi H, Morito K, Masamune Y, Kasugai S, Yokogawa K, Miyamoto K. Novel drug delivery system to bone using acidic oligopeptide: pharmacokinetic characteristics and pharmacological potential. J Drug Target. 2001;9(2):111–21.
25. Jiang T, Yu X, Carbone EJ, Nelson C, Kan HM, Lo KW. Poly aspartic acid peptide-linked PLGA based nanoscale particles: potential for bone-targeting drug delivery applications. Int J Pharm. 2014;475(1–2):547–57.
26. Anderson PS, Rodan GA, Thompson DD, Thompson WJ. Polymalonic acids as boneaffinity agents. In.: EP; 1989.
27. Perrin DD. Binding of Tetracyclines to Bone. Nature. 1965;208(5012):787–8.
28. Xie Y, Liu C, Huang H, Huang J, Deng A, Zou P, Tan X. Bone-targeted delivery of simvastatin-loaded PEG-PLGA micelles conjugated with tetracycline for osteoporosis treatment. Drug Deliv Transl Res. 2018;8(5):1090–102.
29. Lin X, Wang Q, Gu C, Li M, Chen K, Chen P, Tang Z, Liu X, Pan H, Liu Z, Tang R, Fan S. Smart nanosacrificial layer on the bone surface prevents osteoporosis through acid-base neutralization regulated biocascade effects. J Am Chem Soc. 2020;142(41):17543–56.
30. Zhang X, Ji A, Wang Z, Lou H, Li J, Zheng L, Zhou Y, Qu C, Liu X, Chen H, Cheng Z. Azide-dye unexpected bone targeting for near-infrared window ii osteoporosis imaging. J Med Chem. 2021;64(15):11543–53.
31. Hughes DE, Wright KR, Uy HL, Sasaki A, Yoneda T, Roodman GD, Mundy GR, Boyce BF. Bisphosphonates promote apoptosis in murine osteoclasts in vitro and in vivo. J Bone Miner Res. 1995;10(10):1478–87.
32. Fisher JE, Rogers MJ, Halasy JM, Luckman SP, Hughes DE, Masarachia PJ, Wesolowski G, Russell RG, Rodan GA, Reszka AA. Alendronate mechanism of action: geranylgeraniol, an intermediate in the mevalonate pathway, prevents inhibition of osteoclast formation, bone resorption, and kinase activation in vitro. Proc Natl Acad Sci U S A. 1999;96(1):133–8.
33. Qiao W, Lan X, Tsoi JKH, Chen Z, Su RYX, Yeung Kelvin WK, Matinlinna JP. Biomimetic hollow mesoporous hydroxyapatite microsphere with controlled morphology, entrapment efficiency and degradability for cancer therapy. RSC Adv. 2017;7(71):44788–98.
34. Lan X, Zhu W, Huang X, Yu Y, Xiao H, Jin L, Pu JJ, Xie X, She J, Lui VWY, Chen HJ, Su YX. Microneedles loaded with anti-PD-1-cisplatin nanoparticles for synergistic cancer immunochemotherapy. Nanoscale. 2020;12(36):18885–98.
35. Green JR, Clézardin P. Mechanisms of bisphosphonate effects on osteoclasts, tumor cell growth, and metastasis. Am J Clin Oncol. 2002;25(6 Suppl 1):S3-9.
36. Russell R. Determinants of structure–function relationships among bisphosphonates. Bone. 2007;40(5-supp-S2):S21-S25.
37. Ryu TK, Kang RH, Jeong KY, Jun DR, Koh JM, Kim D, Bae SK, Choi SW. Bone-targeted delivery of nanodiamond-based drug carriers conjugated with alendronate for potential osteoporosis treatment. J Control Release. 2016;232:152–60.
38. Lan X, She J, Lin D-A, Xu Y, Li X, Yang W-F, Lui VWY, Jin L, Xie X, Su Y-X. Microneedle-mediated delivery of lipid-coated cisplatin nanoparticles for efficient and safe cancer therapy. ACS Applied Materials & Interfaces. 2018;10(39):33060–33069.
39. Yin H, Kanasty RL, Eltoukhy AA, Vegas AJ, Dorkin JR, Anderson DG. Non-viral vectors for gene-based therapy. Nat Rev Genet. 2014;15(8):541–55.
40. Noble GT, Stefanick JF, Ashley JD, Kiziltepe T, Bilgicer B. Ligand-targeted liposome design: challenges and fundamental considerations. Trends Biotechnol. 2014;32(1):32–45.
41. Hou X, Zaks T, Langer R, Dong Y. Lipid nanoparticles for mRNA delivery. Nat Rev Mater. 2021;6(12):1078–94.
42. Nakagawa O, Ming X, Huang L, Juliano RL. Targeted intracellular delivery of antisense oligonucleotides via conjugation with small-molecule ligands. J Am Chem Soc. 2010;132(26):8848–9.
43. Radwan AA, Alanazi FK. Targeting cancer using cholesterol conjugates. Saudi Pharm J. 2014;22(1):3–16.
44. Mehnath S, Karthikeyan K, Rajan M, Jeyaraj M. Fabrication of bone-targeting hyaluronic acid coupled alendronate-bioactive glass for osteosarcoma therapy. Mater Chem Phys. 2021;273:125146.
45. Cole LE, Vargo-Gogola T, Roeder RK. Targeted delivery to bone and mineral deposits using bisphosphonate ligands. Adv Drug Deliv Rev. 2016;99(Pt A):12–27.
46. Hengartner MO. The biochemistry of apoptosis. Nature. 2000;407(6805):770–6.
47. Mialou V, Philip T, Kalifa C, Perol D, Gentet JC, Marec-Berard P, Pacquement H, Chastagner P, Defaschelles AS, Hartmann O. Metastatic osteosarcoma at diagnosis: prognostic factors and long-term outcome–the French pediatric experience. Cancer. 2005;104(5):1100–9.
48. Chen S, Jin Z, Dai L, Wu H, Wang J, Wang L, Zhou Z, Yang L, Gao W. Aloperine induces apoptosis and inhibits invasion in MG-63 and U2OS human osteosarcoma cells. Biomed Pharmacother. 2018;97:45–52.
49. Huang L, Huang Z, Lin W, Wang L, Zhu X, Chen X, Yang S, Lv C. Salidroside suppresses the growth and invasion of human osteosarcoma cell lines MG63 and U2OS in vitro by inhibiting the JAK2/STAT3 signaling pathway. Int J Oncol. 2019;54(6):1969–80.
50. Seyfert UT, Biehl V, Schenk J. In vitro hemocompatibility testing of biomaterials according to the ISO 10993–4. Biomol Eng. 2002;19(2–6):91–6.